Bol. Soc. Paran. Mat.
©SPM – E-ISSN-2175-1188
SPM: www.spm.uem.br/bspm

(3s.) **v. 2025 (43)** : 1–19.
ISSN-0037-8712
doi:10.5269/bspm.62635

An efficient difference scheme based on cubic B-spline Quasi-interpolation for a time fractional partial integro-differential equation with a weakly singular kernel

Mehran Taghipour and Hossein Aminikhah

ABSTRACT: In this paper, a difference scheme based on cubic B–spline Quasi–interpolation has been derived for the solution of a time fractional partial integro–differential equation with a weakly singular kernel. The fractional derivative of the mentioned equation has been described in the Riemann–Liouville sense. Time fractional derivative is approximated by a scheme of order $O(\tau^2)$. The spatial second derivative has been approximated using the second derivative of the cubic B–spline Quasi–interpolation. We show that the proposed scheme is uniquely solvable, stable and convergent. It has also been shown that the method is the convergence of order $O(\tau^{\frac{3}{2}} + h^2)$. Numerical experiments are provided to verify the effectiveness of the proposed method.

Key Words: Time fractional partial integro-differential equation, Cubic B-spline Quasi-interpolation, Finite difference, Riemann-Liouville derivative, Stability, Convergence.

Contents

1. Introduction

The concept of a fractional derivative firstly appeared in a letter written to L'Hopital by Leibniz in 1695 [1,2,4,6,7,3,5]. In recent years, the Fractional calculus has gained the increasing attention of many researchers. For the description of memory and some physical properties of various materials and processes, modeling with fractional derivatives is very appropriate. This is the main benefit of fractional derivatives in comparison with classical integer order models, in which such effects are missed [8,9,10,11]. Also, the fractional model is employed to achieve a performance that would otherwise be hard to come by [12].

Fractional differential equations have been vastly used in various fields such as control theory [13,14], physics [15,16], engineering [19,20,17,18], geophysics [21], health science [22] and etc. There are some excellent books about fractional calculus and fractional differential equations such as [8,23,24].

There are many numerical methods proposed for solving the fractional differential equations up till now, e.g., finite element methods [25,26,27], finite difference methods [28,29,30], spectral methods [31,32] and etc. Also numerical methods for fractional differential equations can be found in books [24,33,34].

The finite difference method is widely used for the solution of linear and nonlinear differential equations governing science problems. Finite difference methods are simple to formulate, can readily be extended to two or three-dimensional problems, are easy to learn and apply [35,36].

Spline is a special function defined piecewise by polynomials. The spline approximation first appeared in a paper by Schoenberg [37]. Spline interpolation is a form of interpolation where the interpolant is a

Submitted February 22, 2022. Published March 24, 2025
2010 *Mathematics Subject Classification:* 65M12, 65M70, 65R10.

special type of piecewise polynomial called a spline. More details about splines can be found in references [38,39,40].

In 1835 Liouville considered the fractional derivative of function $f(x)$, denoted by $D^{\alpha}f(x)$, of order α [41]. After him, Riemann, Grunwald, Hadamard, Caputo, Agrawal, Riesz, Osler, Prabhakar, Hilfer and etc proposed definitions of the fractional derivatives. A review of definitions for fractional derivatives can be found in [42].

In this paper, we consider the following time fractional partial integro–differential equation with a weakly singular kernel

$$ {}_0^{RL}D_t^{\alpha}u(x,t) = \gamma u_{xx}(x,t) + \int_0^t (t-s)^{-\frac{1}{2}} u_{xx}(x,s)ds + f(x,t) \;\; a \le x \le b,\; 0 \le t \le T, \tag{1.1}$$

where $\gamma \ge 0$ and $f(x,t)$ is a known function, boundary conditions are

$$ u(a,t) = u(b,t) = 0, \;\; 0 \le t \le T. \tag{1.2}$$

initial conditions

$$ u(x,0) = g(x), \tag{1.3}$$

and ${}_0^{RL}D_t^{\alpha}u(x,t)$ denotes the Rieman–Liouville fractional derivative of $u(x,t)$ in time t, given by

$$ {}_0^{RL}D_t^{\alpha}u(x,t) = \frac{1}{\Gamma(1-\alpha)}\frac{d}{dt}\int_0^t \frac{u(x,t)}{(t-s)^{\alpha}}ds. \tag{1.4}$$

Partial integro–differential equations with a weakly kernel have many applications in physics and chemical reactions, such as heat conduction, strerology and etc [43].

Fractional integro–differential equations with a weakly singular kernel has been studied by many researchers. Mohebbi [44] developed a compact finite difference for the solution of time fractional partial integro–differential equation with a weakly singular kernel. Abbaszadeh and Dehghan [45] proposed an efficient numerical technique for solving space time fractional partial weakly singular integro–differential equation. In [46] a numerical solution of the fourth order partial integro–differential equation with multi term kernels by the sinc collocation method based on the double exponential transformation is introduced and analyzed. Wang [47] derived sharp error estimate of a compact L1–ADI scheme for the tow dimensional time fractional integro–differential equation with singular kernel. Qiao [48] proposed an ADI difference scheme based on fractional trapezoidal rule for fractional integro–differential equation with a weakly singular kernel. Xu [49] derived a compact finite difference scheme for the fourth–order time fractional integro–differential equation with a weakly singular kernel.

In the present paper, we propose a finite difference scheme using cubic B–spline Quasi—interpolation to solve (1.1)-(1.3). The solvability, stability, and convergence of the method are proven.

The remainder of the paper is organized as follows. In section 2, we introduce some basic concepts about Quasi–interpolants. In section 3, we proposed a difference scheme using cubic B–spline Quasi–interpolation to solve a time fractional partial integro–differential equation with a weakly singular kernel. The stability and convergence of the scheme are given in sections 4,5. Some numerical examples are presented in section 6. Some conclusions are outlined in the last section.

2. Univariate Spline Quasi–Interpolants

In this section, we introduce the basic concepts about B–spline and univariate B–spline Quasi–interpolants that we will use in the next section.

According to [38] let

$$ P_d^1 := space\ of\ univariate\ polynomials\ of\ degree\ at\ most\ d \tag{2.1}$$

and, $\Omega = [a,b]$ be an interval that has been partitioned into subintervals via a set of points $\Delta = \{x_i\}_{i=0}^{k+1}$ with

$$ a = x_0 < x_1 < \cdots < x_k < x_{k+1} = b. \tag{2.2}$$

We define the space of univariate polynomial splines of smoothness r and degree d with knots Δ as

$$\mathcal{S}_d^r(\Delta) := \{s \in C^r(\Omega) : s\big|_{(x_i,x_{i+1})} \in P_d^1, i = 0,\dots,k\}, \tag{2.3}$$

where $0 \le r < d$ are given integers. We have

$$n := dim\ \mathcal{S}_d^r(\Delta) = k(d-r) + r + 1. \tag{2.4}$$

For a formal proof of this fact, see Theorem 4.4 of [39].

Given $0 \le r < d$ and $\Delta = \{x_i\}_{i=0}^{k+1}$, the associated extended partition Δ_e is defined to be $\{y_i\}_{i=0}^{n+d+1}$, where n is the dimension of $\mathcal{S}_d^r(\Delta)$ given in (2.3),

$$a = y_1 = \cdots = y_{d+1}, \quad y_{n+1} = \cdots = y_{n+d+1} = b, \tag{2.5}$$

and

$$y_{d+2} \le \cdots \le y_n = \overbrace{x_1,\dots,x_1}^{d-r},\dots,\overbrace{x_k,\dots,x_k}^{d-r}. \tag{2.6}$$

Given an extended partition Δ_e, let

$$Q_i^1(t) := \begin{cases} \frac{1}{y_{i+1}-y_i}, & y_i \le t < y_{i+1}, \\ 0, & otherwise, \end{cases} \tag{2.7}$$

for $i = 1,\dots,n+d$, and let

$$Q_i^m(t) := \begin{cases} \frac{(t-y_i)Q_i^{m-1}(t)+(y_{i+m}-t)Q_{i+1}^{m-1}(t)}{y_{i+m}-y_i}, & y_i \le t < y_{i+m}, \\ 0, & otherwise, \end{cases} \tag{2.8}$$

for $2 \le m \le d+1$ and $i = 1,\dots,n+d-m+1$. Let

$$N_i^m(t) := (y_{i+m} - y_i)Q_i^m(t), \quad i = 1,\dots,n+d-m+1. \tag{2.9}$$

We call these the normalized B–splines of order m (or degree $m-1$) associated with the extended partition Δ_e.

In [38], univariate B–spline Quasi–interpolants can be defined as a fourmula of the form

$$Q_d f(x) = \sum_{i=1}^{n+d} (\lambda_i f) N_i(x). \tag{2.10}$$

where $\{N_i\}_{i=1}^{n+d}$ are the B–splines forming a basis of $\mathcal{S}_d^r(\Delta)$.

Quasi–interpolants have been heavily studied in the literature. Some basic ideas and sources for further information can be found in [50]. For a good approximations, we need to make sure it reproduces polynomials, i.e., $Qp = p$ for all $p \in P_d^1$. For each $i = 1,\dots,n$ we assume that the coefficient λ_i is a linear functional defined on $C[a,b]$ that can be computed from samples of f at some set of points $\sigma(\lambda_i)$ in $[a,b]$.

According to [40] the error of a Quasi–interpolation satisfies

$$|f(x) - (Q_d f)(x)| \le \frac{\|Q_d\|}{(d+1)!} \|f^{(d+1)}\|_{\infty,D_x} h(x)^{d+1}, x \in D_y^d, \tag{2.11}$$

where $D_y^d = [y_{d+1}, y_{n+1}]$, D_x is the union of the supports of all B–splines N_i, $i \sim x$ and $\|f^{(d+1)}\|_{\infty,D_x}$ denotes the maximum norm of $f^{(d+1)}$ on D_x and $h(x) = \max_{y\in D_x} |y-x|$ that $\sim$ is used to indicate proportionality. If the local mesh ratio is bounded, i.e., if the quotients of the lengths of adjacent knot intervals are $\le r_y$, then the error of the derivatives on the knot intervals (y_l, y_{l+1}) can be estimated by

$$|f^{(j)}(x) - (Q_d f)^{(j)}(x)| \le c(d, r_y)\|Q_d\| \|f^{(d+1)}\|_{\infty,D_x} h(x)^{d+1-j}, \tag{2.12}$$

for $j \leq d$.

Suppose $a = t_0 < \cdots < t_n = b$ are equally spaced points in the interval $[a, b]$. Let

$$\lambda_i f := \begin{cases} f(t_0), & i = 1, \\ \frac{1}{18}(7f(t_0) + 18f(t_1) - 9f(t_2) + 2f(t_3)), & i = 2, \\ \frac{1}{6}(-f(t_{i-3}) + 8f(t_{i-2}) - f(t_{i-1})), & 3 \leq i \leq n+1, \\ \frac{1}{18}(2f(t_{n-3}) - 9f(t_{n-2}) + 18f(t_{n-1}) + 7f(t_n)), & i = n+2, \\ f(t_n), & i = n+3. \end{cases} \tag{2.13}$$

Then (2.10) defines a linear operator mapping $C[a, b]$ into $\mathcal{S}_3^2(\Delta)$ with $Qp = p$ for all cubic polynomials p. For approximate derivatives of f by derivatives of $Q_3 f$ up to the order h^3, we can evaluate the value of f' and f'' at x_i by $(Q_3 f)'(x) = \sum_{i=1}^{n+3} (\lambda_i f) N_i^{'}(x)$ and $(Q_3 f)''(x) = \sum_{i=1}^{n+3} (\lambda_i f) N_i^{''}(x)$. We set $Y = (f_0, f_1, \ldots, f_n)^T$, $Y' = (f_0', f_1', \ldots, f_n')^T$ and $Y'' = (f_0'', f_1'', \ldots, f_n'')^T$ where $f_j^{'} = (Q_3 f)'(x_j)$, $j = 1, \ldots, n$ and $f_j^{''} = (Q_3 f)''(x_j)$, $j = 1, \ldots, n$. By solution of the linear systems

$$f_i^{'} = \sum_{i=1}^{n+3} (\lambda_i f) N_i^{'}(x), \quad i = 0, 1, \ldots, n, \tag{2.14}$$

$$f_i^{''} = \sum_{i=1}^{n+3} (\lambda_i f) N_i^{''}(x), \quad i = 0, 1, \ldots, n, \tag{2.15}$$

we obtain

$$Y^{'} = \frac{1}{h} D_1 Y, \quad Y^{''} = \frac{1}{h^2} D_2 Y, \tag{2.16}$$

where $D_1, D_2 \in \mathbb{R}^{(n+1)\times(n+1)}$ are obtained as follows:

$$D_1 = \begin{pmatrix} -\frac{11}{6} & 3 & -\frac{3}{2} & \frac{1}{3} & 0 & 0 & \ldots & 0 & 0 \\ -\frac{1}{3} & -\frac{1}{2} & 1 & -\frac{1}{6} & 0 & 0 & \ldots & 0 & 0 \\ \frac{1}{12} & -\frac{2}{3} & 0 & \frac{2}{3} & -\frac{1}{12} & 0 & \ldots & 0 & 0 \\ 0 & \frac{1}{12} & -\frac{2}{3} & 0 & \frac{2}{3} & -\frac{1}{12} & \ldots & 0 & 0 \\ \vdots & \vdots & \vdots & \vdots & \vdots & \vdots & \vdots & \vdots & \vdots \\ 0 & 0 & \ldots & \frac{1}{12} & -\frac{2}{3} & 0 & \frac{2}{3} & -\frac{1}{12} & 0 \\ 0 & 0 & \ldots & 0 & \frac{1}{12} & -\frac{2}{3} & 0 & \frac{2}{3} & -\frac{1}{12} \\ 0 & 0 & \ldots & 0 & 0 & \frac{1}{6} & -1 & \frac{1}{2} & \frac{1}{3} \\ 0 & 0 & \ldots & 0 & 0 & -\frac{1}{3} & \frac{3}{2} & -3 & \frac{11}{6} \end{pmatrix},$$

$$D_2 = \begin{pmatrix} 2 & -5 & 4 & -1 & 0 & 0 & \ldots & 0 & 0 \\ 1 & -2 & 1 & 0 & 0 & 0 & \ldots & 0 & 0 \\ -\frac{1}{6} & \frac{5}{3} & -3 & \frac{5}{3} & -\frac{1}{6} & 0 & \ldots & 0 & 0 \\ 0 & -\frac{1}{6} & \frac{5}{3} & -3 & \frac{5}{3} & -\frac{1}{6} & \ldots & 0 & 0 \\ \vdots & \vdots & \vdots & \vdots & \vdots & \vdots & \vdots & \vdots & \vdots \\ 0 & 0 & \ldots & -\frac{1}{6} & \frac{5}{3} & -3 & \frac{5}{3} & -\frac{1}{6} & 0 \\ 0 & 0 & \ldots & 0 & -\frac{1}{6} & \frac{5}{3} & -3 & \frac{5}{3} & -\frac{1}{6} \\ 0 & 0 & \ldots & 0 & 0 & 0 & 1 & -2 & 1 \\ 0 & 0 & \ldots & 0 & 0 & -1 & 4 & -5 & 2 \end{pmatrix}.$$

3. Numerical method

The domain is divided into a uniform grid of mesh points (x_j, t_k) with $x_j = a + jh$, $h = \frac{b-a}{M}$, $0 \leq j \leq M$ and $t_k = k\tau$, $\tau = \frac{T}{N}$, $0 \leq k \leq N$. The values of the function u at the grid points are denoted $u(x_m, t_k)$ and U_m^k is the approximate solution at the point (x_m, t_k).

For the approximation of the Riemann-Liouville fractional derivative, we have the following lemma.

Lemma 3.1 *[51,52] Let $\alpha \in (0,1)$ then the following second-order weighted and shifted Grunwald difference (WSGD) approximation formula holds*

$$ {}_0^{RL}D_t^{\alpha}u(x,t_k) = \tau^{-\alpha}\sum_{j=0}^{k}\lambda_j^{(\alpha)}u(x,t_{k-j}) + O(\tau^2), \tag{3.1}$$

in which

$$\lambda_j^{(\alpha)} = \begin{cases} \frac{2+\alpha}{2}, & j=0, \\ \frac{2+\alpha}{2}g_j^{(\alpha)} - \frac{\alpha}{2}g_{j-1}^{(\alpha)}, & j \geq 1, \end{cases}$$

where

$$g_0^{(\alpha)} = 1,\ g_1^{(\alpha)} = -\alpha,\ g_j^{(\alpha)} = \frac{\Gamma(j-\alpha)}{\Gamma(-\alpha)\Gamma(j+1)},\ j \geq 2.$$

Let $I(f,t) = \int_0^t (t-s)^{-\frac{1}{2}} f(s)ds$, then according to [53] we have the following approximation

$$I(f,t_k) = A_k f(t_0) + \sum_{p=0}^{k}\beta_p f(t_{k-p}) + O(\tau^{\frac{3}{2}}),\ \ 1 \leq k \leq N, \tag{3.2}$$

where

$$\begin{aligned} A_k &= 2\big[t_k^{\frac{1}{2}} - \frac{2}{3\tau}(t_{k+1}^{\frac{3}{2}} - t_k^{\frac{3}{2}})\big],\ \ \beta_0 = \frac{4}{3\tau}(t_1^{\frac{3}{2}}) + \frac{4\sqrt{\tau}}{3}\beta, \\ \beta_1 &= \frac{4}{3\tau}\big[t_2^{\frac{3}{2}} - 2t_1^{\frac{3}{2}} + t_0^{\frac{3}{2}}\big] - \frac{4\sqrt{\tau}}{3}\beta, \\ \beta_p &= \frac{4}{3\tau}\big[t_{p+1}^{\frac{3}{2}} - 2t_p^{\frac{3}{2}} + t_{p-1}^{\frac{3}{2}}\big]\ \ p \geq 2, \end{aligned} \tag{3.3}$$

and β is a nonnegative constant and is dependent of τ and h.

Now, we present a finite difference scheme for solving (1.1)-(1.3) based on cubic B–spline Quasi–interpolant. We approximate equation (1.1) at the point (x_j,t_k) by (3.1) and (3.2)

$$\tau^{-\alpha}\sum_{j=0}^{k}\lambda_j^{(\alpha)}u(x,t_{k-j}) = \gamma u_{xx}(x_j,t_k) + A_k u_{xx}(x_j,t_0) + \sum_{p=0}^{k}\beta_p u_{xx}(x_j,t_{k-p}) + f_j^k + R^k. \tag{3.4}$$

Now using (2.16) we have

$$\tau^{-\alpha}\sum_{j=0}^{k}\lambda_j^{(\alpha)}u_j^{k-j} = \frac{\gamma}{h^2}\sum_{l=0}^{M}d_{jl}u_l^k + \frac{A_k}{h^2}\sum_{l=0}^{M}d_{jl}u_l^0 + \sum_{p=0}^{k}\frac{\beta_p}{h^2}\sum_{l=0}^{M}d_{jl}u_l^{k-p} + f_j^k + R^k, \tag{3.5}$$

where $R^k = O(\tau^{\frac{3}{2}} + h^2)$. Therefore by ignoring R^k we have

$$h^2\tau^{-\alpha}\lambda_0^{(\alpha)}U_j^k - (\gamma+\beta_0)\sum_{l=0}^{M}d_{jl}U_l^k = A_k\sum_{l=0}^{M}d_{jl}U_l^0 + \sum_{p=1}^{k}\sum_{l=0}^{M}\beta_p d_{jl}U_l^{k-p} - h^2\tau^{-\alpha}\sum_{j=1}^{k}\lambda_j^{(\alpha)}U_j^{k-j} + h^2 f_j^k, \tag{3.6}$$

where $1 \leq k \leq N$ and $1 \leq j \leq M-1$.

We set $\mu = \gamma + \beta_0$ and $\sigma = h^2\tau^{-\alpha}\lambda_0^{(\alpha)}$, so that in each time step we solve the following pentadiagonal system of linear equations

$$AU^k = F^k, \tag{3.7}$$

where

$$A=\begin{pmatrix} \sigma+2\mu & -\mu & 0 & 0 & 0 & 0 & \dots & 0 & 0 \\ -\frac{5}{3}\mu & \sigma+3\mu & -\frac{5}{3}\mu & \frac{1}{6}\mu & 0 & 0 & \dots & 0 & 0 \\ \frac{1}{6}\mu & -\frac{5}{3}\mu & \sigma+3\mu & -\frac{5}{3}\mu & \frac{1}{6}\mu & 0 & \dots & 0 & 0 \\ \vdots & \vdots & \vdots & \vdots & \vdots & \vdots & \vdots & \vdots & \vdots \\ 0 & 0 & \dots & 0 & \frac{1}{6}\mu & -\frac{5}{3}\mu & \sigma+3\mu & -\frac{5}{3}\mu & \frac{1}{6}\mu \\ 0 & 0 & \dots & 0 & 0 & \frac{1}{6}\mu & -\frac{5}{3}\mu & \sigma+3\mu & -\frac{5}{3}\mu \\ 0 & 0 & \dots & 0 & 0 & 0 & 0 & -\mu & \sigma+2\mu \end{pmatrix}, U^{k+1}=\begin{pmatrix} U_1^k \\ U_2^k \\ U_3^k \\ \vdots \\ U_{M-3}^k \\ U_{M-2}^k \\ U_{M-1}^k \end{pmatrix},$$

$$F^k=\begin{pmatrix} A_k\sum_{l=0}^{M} d_{1l}U_l^0+\sum_{p=0}^{k}\sum_{l=0}^{M}\beta_p d_{1l}U_l^{k-p}-h^2\tau^{-\alpha}\sum_{j=1}^{k}\lambda_j^{(\alpha)}U_1^{k-j}+h^2f_1^k+\mu U_0^k \\ A_k\sum_{l=0}^{M} d_{2l}U_l^0+\sum_{p=0}^{k}\sum_{l=0}^{M}\beta_p d_{1l}U_2^{k-p}-h^2\tau^{-\alpha}\sum_{j=1}^{k}\lambda_j^{(\alpha)}U_2^{k-j}+h^2f_2^k-\frac{1}{6}\mu U_0^k \\ A_k\sum_{l=0}^{M} d_{3l}U_l^0+\sum_{p=0}^{k}\sum_{l=0}^{M}\beta_p d_{1l}U_3^{k-p}-h^2\tau^{-\alpha}\sum_{j=1}^{k}\lambda_j^{(\alpha)}U_3^{k-j}+h^2f_3^k \\ \vdots \\ A_k\sum_{l=0}^{M} d_{M-2l}U_l^0+\sum_{p=0}^{k}\sum_{l=0}^{M}\beta_P d_{M-2l}U_l^{k-p}-h^2\tau^{-\alpha}\sum_{j=1}^{k}\lambda_j^{(\alpha)}U_{M-2}^{k-j}+h^2f_{M-2}^k-\frac{1}{6}\mu U_M^k \\ A_k\sum_{l=0}^{M} d_{M-1l}U_l^0+\sum_{p=0}^{k}\sum_{l=0}^{M}\beta_P d_{M-1l}U_l^{k-p}-h^2\tau^{-\alpha}\sum_{j=1}^{k}\lambda_j^{(\alpha)}U_{M-1}^{k-j}+h^2f_{M-1}^k+\mu U_M^k \end{pmatrix}.$$

Now we give the solvability of scheme (3.6).

Theorem 3.1 *If $h^2>\frac{4\mu\tau^\alpha}{3(2+\alpha)}$, then the coefficient matrices in linear system (3.7) is invertible.*

Proof: According to the condition $h^2>\frac{4\mu\tau^\alpha}{3(2+\alpha)}$ we have

$$\left|\sigma+3\mu\right|=\sigma+3\mu>\frac{4}{3}\frac{\mu}{2+\alpha}\frac{2+\alpha}{2}+3\mu=\frac{2}{3}\mu+3\mu=\left|\frac{1}{6}\mu\right|+\left|-\frac{5}{3}\mu\right|+\left|-\frac{5}{3}\mu\right|+\left|\frac{1}{6}\mu\right|,$$

so that the cofficient matrices are strictly diagonally dominant. Thus these matrices are invertible. □

4. Stability

To study the stability analysis of the proposed scheme, we use the Fourier method. This method is a very useful technique for analyzing the stability of a finite difference method. It uses mutually orthogonal vectors that form a basis for n-dimensional space. Thus the error term can be expanded as a linear combination of these basis vectors. Let $\tilde{U}_j^k$ be the approximate solution of the scheme, and define

$$\zeta_j^k=U_j^k-\tilde{U}_j^k,\qquad 1\le j\le M-1,\quad 1\le k\le N,$$

with corresponding vector

$$\zeta^k=(\zeta_1^k,\zeta_2^k,\dots,\zeta_{M-1}^k)^T.$$

Thus for $k\ge 1$ we have

$$\sigma\zeta_j^k-\mu\sum_{l=0}^{M}d_{jl}\zeta_l^k=A_k\sum_{l=1}^{k}d_{jl}\zeta_j^0+\sum_{p=1}^{k}\sum_{l=0}^{M}\beta_P d_{jl}\zeta_j^{k-p}-\tau^{-\alpha}h^2\sum_{l=1}^{k}\lambda_j^{(\alpha)}\zeta_j^{k-l}. \tag{4.1}$$

Now we define the grid functions as follows:

$$\zeta^k(x)=\begin{cases}\zeta_j^k, & x_j-\frac{h}{2}<x\le x_j+\frac{h}{2},\\ 0, & 0\le x\le\frac{h}{2}orL-\frac{h}{2}<x\le L.\end{cases} \tag{4.2}$$

We can expand $\zeta^k(x)$ into a Fourier series

$$\zeta^k(x) = \sum_{l=-\infty}^{\infty} d_k(l) e^{i2\pi lx/L}, \tag{4.3}$$

where

$$d_k(l) = \frac{1}{L}\int_0^L \zeta^k(x) e^{-i2\pi lx/L}\,\mathrm{d}x. \tag{4.4}$$

Denoting

$$\|\zeta^k\|_2 = \left(\int_0^L \|\zeta^k(x)\|^2\,\mathrm{d}x\right)^{\frac{1}{2}}, \tag{4.5}$$

and using the Parseval equality

$$\int_0^L \|\zeta^k(x)\|^2\,\mathrm{d}x = \sum_{l=-\infty}^{\infty} \|d_k(l)\|^2, \tag{4.6}$$

one has

$$\|\zeta^k\|^2 = \sum_{l=-\infty}^{\infty} \|d_k(l)\|^2. \tag{4.7}$$

We can expand ζ_j^k into Fourier series, and Because the difference equations are linear, we can analyze the behavior of the total error by tracking the behavior of an arbitrary nth component. So we can suppose that the solution of (4.1) has the following form

$$\zeta_j^k = d_k e^{i\sigma_x jh},$$

where $\sigma_x = 2\pi l/L$. Substituting the above expression into (4.1) we obtain

$$\begin{aligned}\sigma d_k - \mu d_k(-\frac{1}{3}\cos(2\sigma_x h)+\frac{10}{3}\cos(\sigma_x h) - 3) = \sum_{p=1}^{k}\beta_p d_{k-p}(-\frac{1}{3}\cos(2\sigma_x h) + \frac{10}{3}\cos(\sigma_x h) - 3) \\ - \tau^{-\alpha}h^2\sum_{l=1}^{k}\lambda_j^{(\alpha)} d_{k-l} + A_k d_0(-\frac{1}{3}\cos(2\sigma_x h) + \frac{10}{3}\cos(\sigma_x h) - 3).\end{aligned} \tag{4.8}$$

Now if $s = -\frac{1}{3}\cos(2\sigma_x h) + \frac{10}{3}\cos(\sigma_x h) - 3 \le 0$ we have

$$d_k = \frac{s}{\sigma - \mu s}\sum_{p=1}^{k}\beta_p d_{k-p} - \frac{\tau^{-\alpha}h^2}{\sigma - \mu s}\sum_{l=1}^{k}\lambda_j^{(\alpha)} d_{k-l} + \frac{A_k s}{\sigma - \mu s} d_0. \tag{4.9}$$

In order to prove the stability, we need a lemma about the coefficients $\{\lambda_j^{(\alpha)}\}_{j=0}^{\infty}$ and $\{\beta_p\}_{p=0}^{\infty}$.

Lemma 4.1 *[53,52,54] For $\{\lambda_j^{(\alpha)}\}_{j=0}^{\infty}$ defined in lemma (3.1) and $\{\beta_p\}_{p=0}^{\infty}$ defined by (3.3), the following inequality holds for any integer n*

$$\sum_{j=0}^{k+1}|\lambda_j^{(\alpha)}| \le C, \tag{4.10}$$

$$\sum_{p=1}^{k}\beta_p \le C\sqrt{\tau T}. \tag{4.11}$$

Theorem 4.1 *Suppose that d_k, $(1 \le k \le N-1)$ are defined by (4.9). If $\frac{h^2}{\tau^\alpha} \le C$ then for $\alpha \in (0,1)$*

$$|d_k| \leq C_k|d_0|, \quad k = 1, 2, \cdots, N.$$

Proof: We will prove this claim by mathematical induction. For $k = 1$ we have

$$\begin{aligned}|d_1| =& |d_0|\frac{\left|\beta_1 s - \tau^{-\alpha}h^2\lambda_1^{(\alpha)} + A_1 s\right|}{|\mu s - \sigma|} \leq \left(\frac{|\beta_1| + \tau^{-\alpha}h^2|\lambda_1^{(\alpha)}|}{|\mu s - \sigma|} + \frac{|A_1||s|}{|\mu s - \sigma|}\right)|d_0| \\ &\leq |d_0|\frac{C^1\sqrt{\tau}|s|}{|\mu s - \sigma|} + |d_0|\frac{\tau^{-\alpha}h^2|\lambda_1^{(\alpha)}|}{|\mu s - \sigma|} + |d_0|\frac{C^2\sqrt{\tau}|s|}{|\mu s - \sigma|} \\ &\leq C^1|d_0| + C|d_0| + C^2|d_0| = C_1|d_0|.\end{aligned}$$

Assume that

$$|d_k| \leq C_k|d_0|, \quad 1 \leq k \leq N - 2.$$

Using lemma (4.1) we get

$$|d_k| \leq \frac{\sum_{p=1}^{k}|\beta_p||d_{k-p}||s| + \tau^{-\alpha}h^2\sum_{p=1}^{k}|\lambda_p^{(\alpha)}||d_{k-p}|}{|\mu s - \sigma|} + \frac{|d_0||A_k||s|}{|\mu s - \sigma|}.$$

Now assume that

$$C' = \max\{C_0, C_1, \ldots, C_{N-1}\}, \tag{4.12}$$

so

$$\begin{aligned}|d_k| &\leq C'|d_0|\left(\frac{\sum_{p=1}^{k}|\beta_p||s| + \tau^{-\alpha}h^2\sum_{p=1}^{k}|\lambda_p^{(\alpha)}|}{|\mu s - \sigma|} + C^3\right) \\ &\leq C'|d_0|\left(\frac{C^4\sqrt{\tau T} + C^5}{|\mu s - \sigma|} + C^3\right) \leq C_k|d_0|,\end{aligned}$$

This completes the proof. □

Theorem 4.2 *If $\frac{h^2}{\tau^\alpha} \leq C$, the finite difference scheme (3.6) is stable for $\alpha \in (0, 1)$.*

Proof: According to theorem (4.1) and Parseval's equality we obtain

$$\|U^k - \tilde{U}^k\|_{l^2}^2 = \|\zeta^k\|_{l^2}^2 \leq C_k^2\|\zeta^0\|_{l^2}^2,$$

so that

$$\|U^k - \tilde{U}^k\|_{l^2} \leq C\|U^0 - \tilde{U}^0\|_{l^2},$$

which means that the scheme is stable. □

5. Convergence

In this section, we prove that convergence of the difference scheme (3.6). Similar to the previous Section let $e_j^k = u_j^k - U_j^k, 1 \leq j \leq M-1, 0 \leq k \leq N-1$ and and denote, $e^k = (e_1^k, e_2^k, \ldots, e_{M-1}^k)^T, \mathbf{R}^k = (R_1^k, R_2^k, \ldots, R_{M-1}^k)^T, 0 \leq k \leq N-1$.

From Eq. (3.4) and $R_j^{k+1} = O(\tau^2 + h^2)$ and noticing that $e_j^0 = 0$, one has

$$\sigma e_j^k - \mu\sum_{l=0}^{M} d_{jl}e_l^k = \sum_{p=1}^{k}\sum_{l=0}^{M}\beta_P d_{jl}e_j^{k-p} - \tau^{-\alpha}h^2\sum_{l=1}^{k}\lambda_j^{(\alpha)}e_j^{k-l} + R_j^k. \tag{5.1}$$

Using the similar idea of stability analysis, we define the following functions

$$e^k(x) = \begin{cases} e_j^k, & x_j - \frac{h}{2} < x \le x_j + \frac{h}{2}, \ \ 1 \le j \le M-1, \\ 0, & 0 \le x \le \frac{h}{2} \ \ or \ \ L - \frac{h}{2} < x \le L. \end{cases} \tag{5.2}$$

and

$$R^k(x) = \begin{cases} R_j^k, & x_j - \frac{h}{2} < x \le x_j + \frac{h}{2}, \ \ 1 \le j \le M-1, \\ 0, & 0 \le x \le \frac{h}{2} \ \ or \ \ L - \frac{h}{2} < x \le L. \end{cases} \tag{5.3}$$

We expand the $e^k(x)$ and $R^k(x)$ into the following Fourier series expansions

$$e^k(x) = \sum_{l=-\infty}^{\infty} \eta_k(l) e^{i2\pi lx/L}, \ \ R^k(x) = \sum_{l=-\infty}^{\infty} \xi_k(l) e^{i2\pi lx/L}, \tag{5.4}$$

where

$$\eta_k(l) = \frac{1}{L}\int_0^L e^k(x) e^{-i2\pi lx/L}\,\mathrm{d}x, \ \ \xi_k(l) = \frac{1}{L}\int_0^L R^k(x) e^{-i2\pi lx/L}\,\mathrm{d}x. \tag{5.5}$$

Applying the Parseval equality

$$\int_0^L \|e^k(x)\|^2\,\mathrm{d}x = \sum_{l=-\infty}^{\infty} \|\eta_k(l)\|^2, \ \ \int_0^L \|R^k(x)\|^2\,\mathrm{d}x = \sum_{l=-\infty}^{\infty} \|\xi_k(l)\|^2, \tag{5.6}$$

and

$$\int_0^L \|e^k(x)\|^2\,\mathrm{d}x = \sum_{j=1}^{M-1} h\|e_j^k\|^2, \ \ \int_0^L \|R^k(x)\|^2\,\mathrm{d}x = \sum_{j=1}^{M-1} h\|R_j^k\|^2, \tag{5.7}$$

we have

$$\|e^k\|_2^2 = \sum_{l=-\infty}^{\infty} \|\eta_k(l)\|^2, \ \ \|R^k\|_2^2 = \sum_{l=-\infty}^{\infty} \|\xi_k(l)\|^2. \tag{5.8}$$

Now, we suppose that

$$e_j^k = \eta_k e^{i\sigma_x jh},$$
$$R_j^k = \xi_k e^{i\sigma_x jh},$$

where $\sigma_x = \frac{2l\pi}{L}$. Substituting the above relations into (5.1) leads to

$$\eta_k = \frac{s}{\sigma - \mu s}\sum_{p=1}^{k} \beta_p \eta_{k-p} - \frac{\tau^{-\alpha}h^2}{\sigma - \mu s}\sum_{l=1}^{k} \lambda_j^{(\alpha)} \eta_{k-l} + \frac{\xi_k}{\sigma - \mu s}, \ \ 1 \le k \le N-1. \tag{5.9}$$

Theorem 5.1 *If η_k be the solution of Equation (5.9) and $\frac{h^2}{\tau^\alpha} \le C$, then there is positive constant C such that*

$$|\eta_k| \le C|\xi_1|, \ \ k = 1, \ldots, N-1. \tag{5.10}$$

Proof: *We use the mathematical induction for proof. For $k = 1$ from (5.9) and $\eta_0 = 0$ we have*

$$|\eta_1| = \left|\frac{\xi_1}{\sigma - \mu s}\right| \le |\xi_1|.$$

Now, suppose that

$$|\eta_k| \le C|\xi_1|, \ \ k = 1, \ldots, N-2.$$

By using the convergence of the series on the right-hand side of Eq. (5.8), we know that there exists a positive constant C_2, such that

$$|\xi_k| \leq C_2|\xi_1|, \quad k = 1, 2, \ldots, N-1. \tag{5.11}$$

By equation (5.9), we have

$$\begin{aligned} |\eta_{k+1}| &\leq \frac{\sum_{p=1}^{k} |\beta_p||\eta_{k-p}||s| + \tau^{-\alpha}h^2 \sum_{p=1}^{k} |\lambda_p^{(\alpha)}||\eta_{k-p}|}{|\mu s - \sigma|} + \frac{|\xi_k|}{|\mu s - \sigma|} \\ &\leq C|\xi_1|. \end{aligned}$$

□

Theorem 5.2 *If $\frac{h^2}{\tau^\alpha} \leq C$ the difference scheme (3.6) is convergent, and the order of convergence is $O(\tau^{\frac{3}{2}} + h^2)$.*

Proof: By theorem (5.1) and Eq. (5.8), we can obtain

$$\begin{aligned} \|e^k\|_{l^2}^2 = \sum_{l=-\infty}^{\infty} \|\eta_k(l)\|^2 &\leq \sum_{l=-\infty}^{\infty} C^2 \|\xi_1(l)\|^2 \\ &\leq C^2 \sum_{l=-\infty}^{\infty} \|\xi_1(l)\|^2 = C^2 \|R^1\|_{l^2}^2 \\ &\leq C^2 C_1^2 (\tau^{\frac{3}{2}} + h^2)^2 \leq C'^2 (\tau^{\frac{3}{2}} + h^2)^2, \end{aligned}$$

This completes the proof. □

6. Numerical experiments

In this section, we carry out four numerical examples to illustrate the efficiency of the method proposed in this paper. All our tests are performed on a Windows 10 (64 bit) Intel(R) Core(TM) i7-7500U CPU 2.70 GHz, 8.0 GB of RAM using MATLAB R2020b. In all examples we use the error norm

$$\|e(\tau, h)\| = \|e^N\| = \left(\Delta x \sum_{j=1}^{M} (e_j^N)^2 \right)^{\frac{1}{2}},$$

where $e_j^k = u(x_j, t_k) - u_j^k$. We evaluate the convergence order with the following formulas:

$$\begin{aligned} r_1(\tau, h) &= \log_2 \left(\frac{\|e(\tau, 2h)\|}{\|e(\tau, h)\|} \right), \\ r_2(\tau, h) &= \log_2 (\|e(2\tau, h)\| / \|e(\tau, h)\|), \\ r_3(\tau, h) &= \log_2 (\|e(2\tau, 2h)\| / \|e(\tau, h)\|). \end{aligned}$$

Example 6.1 *Consider the time fractional partial integro–differential equation (1.1) with initial and boundary conditions (1.2)-(1.3) with exact solution $u(x, t) = t \sin(\pi x)$. The source term is taken as*

$$f(x, t) = \sin(\pi x) \left(\frac{1}{\Gamma(2-\alpha)} t^{1-\alpha} + \pi^2 t + \frac{4}{3} \pi^2 t^{\frac{3}{2}} \right).$$

In table (1), we calculate errors and convergence orders in spatial direction for difference scheme. We choose different spatial step sizes $h = 1/10, 1/20, \ldots, 1/640$ and fixed temporal step length $\tau = \frac{1}{10}$ to obtain the numerical convergence rates in spatial. The convergence order of the numerical result are in

Table 1: Take $\tau = 0.1$, Error and experiment order of convergence for $\alpha = 0.1, 0.3, 0.5$ for example 6.1

h	$\alpha = 0.1$		$\alpha = 0.3$		$\alpha = 0.5$	
	$\|e^N\|$	$r_1(\tau, h)$	$\|e^N\|$	$r_1(\tau, h)$	$\|e^N\|$	$r_1(\tau, h)$
$\frac{1}{10}$	4.8352e-03		4.8317e-03		4.8348e-03	
$\frac{1}{20}$	1.3632e-03	1.8266	1.3621e-04	1.8267	1.3622e-03	1.8275
$\frac{1}{40}$	3.4646e-04	1.9762	3.4603e-04	1.9769	3.4530e-04	1.9800
$\frac{1}{80}$	8.6230e-05	2.0064	8.5975e-05	2.0090	8.5026e-05	2.0219
$\frac{1}{160}$	2.0910e-05	2.0440	2.0699e-05	2.0543	1.9695e-05	2.1101
$\frac{1}{320}$	4.5668e-06	2.1950	4.3674e-06	2.2447	3.3495e-06	2.5558
$\frac{1}{640}$	4.8041e-07	2.5489	2.8386e-07	3.9435	7.3759e-07	2.1830

Table 2: Error for different h, τ and T for example 6.1

T	h	τ	$\alpha = 0.7$	$\alpha = 0.9$
			$\|e^N\|$	$\|e^N\|$
1	$\frac{1}{100}$	$\frac{1}{100}$	4.8799e-05	2.4758e-05
2	$\frac{1}{1000}$	$\frac{2}{100}$	5.8827e-06	1.9660e-05
4	$\frac{1}{1000}$	$\frac{4}{100}$	4.2864e-06	1.4502e-05
6	$\frac{1}{1000}$	$\frac{6}{100}$	2.7875e-06	1.1210e-05
8	$\frac{1}{1000}$	$\frac{8}{100}$	1.3670e-06	8.6459e-06
10	$\frac{1}{1000}$	$\frac{10}{100}$	1.7378e-09	6.4631e-06
12	$\frac{1}{1000}$	$\frac{12}{100}$	2.5331e-06	4.5117e-06

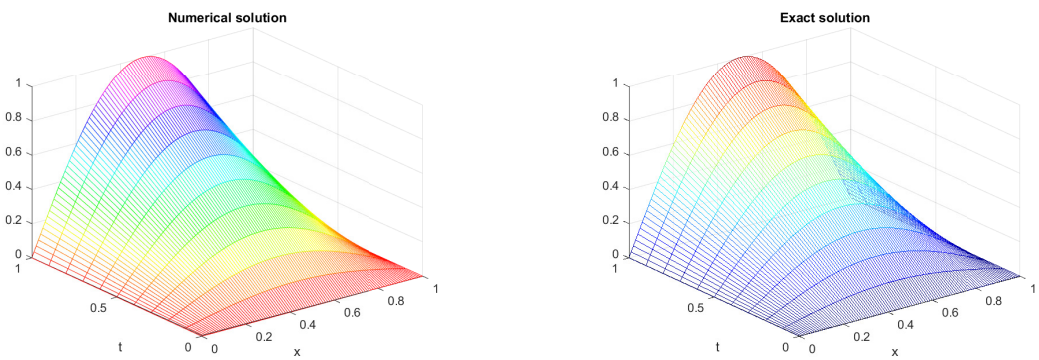

Figure 1: The plot of numerical solution (left) and exact solution (right) at $\tau = 0.1$ and $h = \frac{\pi}{100}$ for example 6.1.

agreement with the results in theorem (5.2). In table (2), we calculate errors at $T = 1, 2, 4, 6, 8, 10, 12$ for different h, τ.

Figure (1) shows the plots of the exact solution and the numerical sulotion computed by difference scheme using $\tau = 0.1$ and $h = \frac{1}{100}$. The plot of pointwise errors and contour plot of numerical solution at $t = 1$ with $\tau = 0.1$ and $h = \frac{1}{100}$ is illustrated in figure (2). In figure (3) a comparison between numerical and exact solution at $t = 1$ with $\tau = 0.1$ and $h = \frac{1}{100}$ is demonstrated. All figures shows that the numerical scheme is efficient .

Example 6.2 *Consider the time fractional partial integro–differential equation (1.1) with initial and boundary conditions (1.2)-(1.3) with exact solution $u(x,t) = t^2(x^2 - 1)$, $(x,t) \in [-1,1] \times [0,1]$. The*

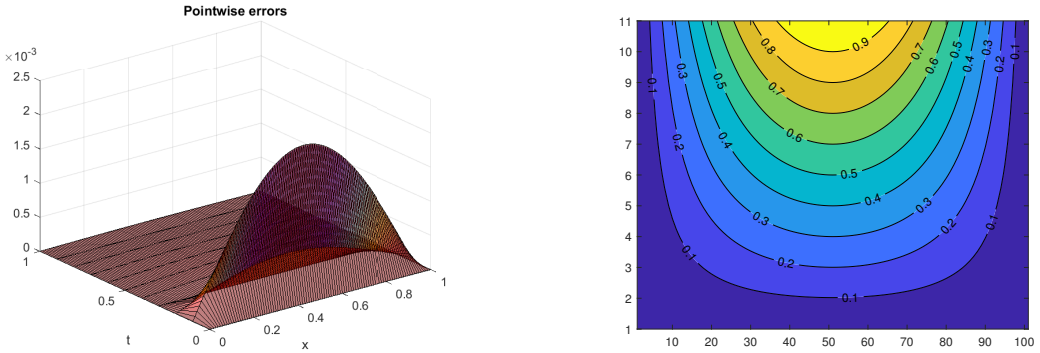

Figure 2: The plot of pointwise errors (left) at $\tau = 0.1$ and $h = \frac{1}{100}$ and contour plot of numerical solution (right) for example 6.1.

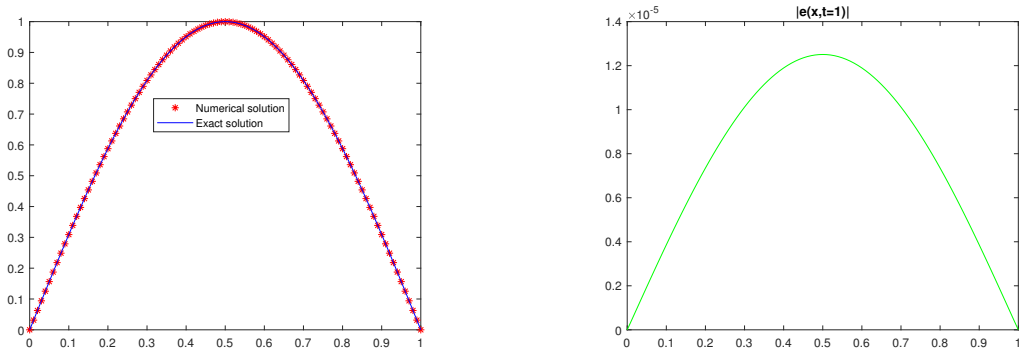

Figure 3: The comparison between numerical solution and exact solution (left) and absolute error (right) with $\tau = 0.1$ and $h = \frac{1}{100}$ at $t = 1$ for example 6.1.

source term is taken as

$$f(x,t) = \frac{2}{\Gamma(3-\alpha)}(x^2-1)t^{2-\alpha} - 2t^2 - \frac{32}{15}t^{\frac{5}{2}}.$$

Table 3: Take $h = 0.1$, Error and experiment order of convergence for $\alpha = 0.1, 0.2, 0.6$ for example 6.2

τ	$\alpha = 0.1$		$\alpha = 0.2$		$\alpha = 0.6$	
	$\|e^N\|$	$r_2(\tau,h)$	$\|e^N\|$	$r_2(\tau,h)$	$\|e^N\|$	$r_2(\tau,h)$
$\frac{1}{10}$	1.004e-03		9.7159e-04		1.0252e-03	
$\frac{1}{20}$	2.5434e-04	1.9757	2.4745e-04	1.9732	2.6263e-04	1.9648
$\frac{1}{40}$	6.4348e-05	1.9828	6.2671e-05	1.9813	6.6764e-05	1.9758
$\frac{1}{80}$	1.6223e-05	1.9878	1.5810e-05	1.9870	1.6883e-05	1.9835
$\frac{1}{160}$	4.0797e-06	1.6752	3.9775e-06	1.9909	4.2542e-06	1.9886

In table (3), we show error norm and convergence orders in temporal direction for difference scheme. We choose different temporal step sizes and fixed spatial step size to obtain the numerical convergence rates in temporal. Figures (4),(7) and (8) shows that the proposed method is efficient.

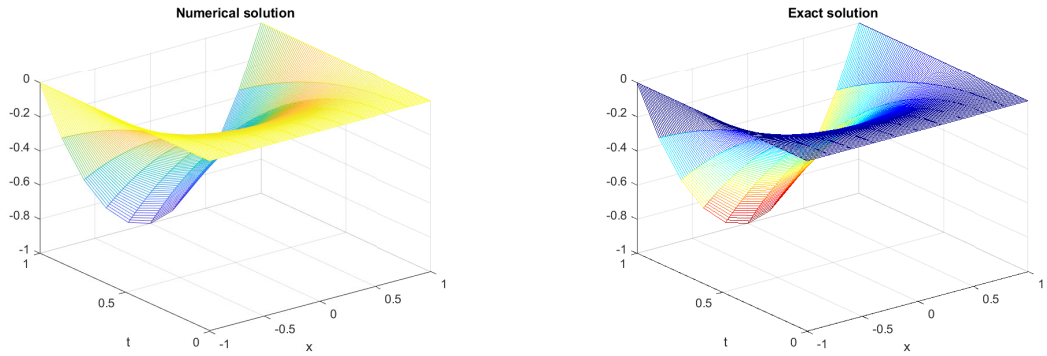

Figure 4: The plot of numerical solution (left) and exact solution (right) at $\tau = 0.01$ and $h = \frac{1}{10}$ for example 6.2.

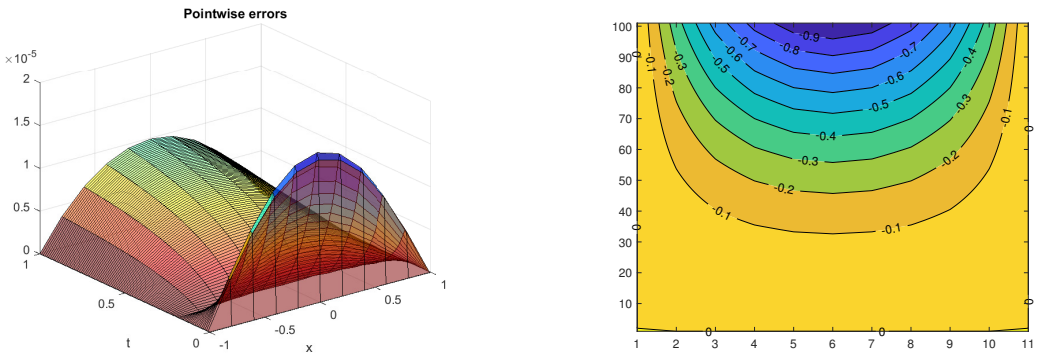

Figure 5: The plot of pointwise errors at $\tau = 0.01$ and $h = \frac{1}{100}$ and contour plot of numerical solution for example 6.2.

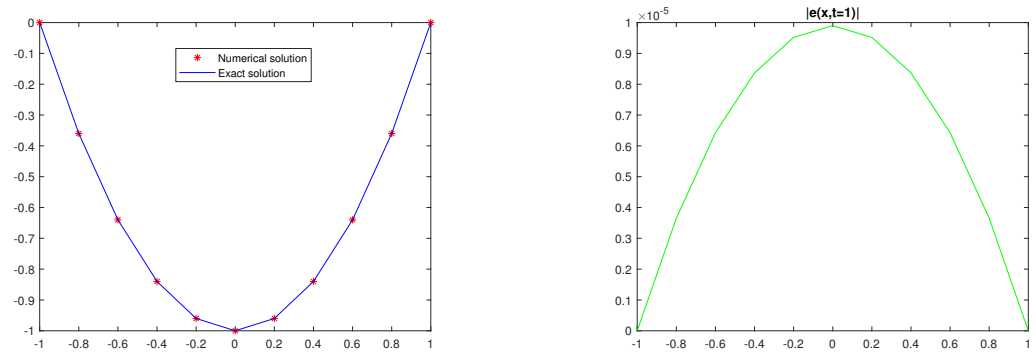

Figure 6: The comparison between numerical solution and exact solution (left) and absolute error (right) with $\tau = 0.01$ and $h = \frac{1}{10}$ at $t = 1$ for example 6.2.

Example 6.3 *Consider the time fractional partial integro–differential equation* (1.1) *with initial and boundary conditions* (1.2)-(1.3) *with exact solution* $u(x,t) = \frac{t^3 \sin(\pi x)}{(x+2)^2}$, $(x,t) \in [0,1] \times [0,1]$. *The source term is taken as*

$$f(x,t)=\frac{6\sin(\pi x)t^{3-\alpha}}{\Gamma(4-\alpha)(2+x)^2}+\left(\frac{\pi^2\sin(\pi x)}{(2+x)^2}-\frac{6\sin(\pi x)}{(2+x)^4}+\frac{4\pi\sin(\pi x)}{(2+x)^3}\right)\left(t^3+\left(\frac{32}{35}\right)t^{\frac{7}{2}}\right).$$

Table 4: Take $\tau=0.1$, Error and experiment order of convergence for $\alpha=0.1,0.3,0.5$ for example 6.3

h	τ	$\alpha=0.1$		$\alpha=0.3$		$\alpha=0.5$	
		$\|e^N\|$	$r_3(\tau,h)$	$\|e^N\|$	$r_3(\tau,h)$	$\|e^N\|$	$r_3(\tau,h)$
$\frac{1}{10}$	$\frac{1}{10}$	6.6155e-04		6.3962e-04		6.1599e-04	
$\frac{1}{20}$	$\frac{1}{20}$	1.9440e-04	1.7668	1.8858e-04	1.7620	1.8233e-04	1.7563
$\frac{1}{40}$	$\frac{1}{40}$	5.0835e-05	1.9351	4.9357e-05	1.9338	4.7779e-05	1.9321
$\frac{1}{80}$	$\frac{1}{80}$	1.2895e-05	1.9790	1.2524e-05	1.9785	1.2129e-05	1.9779
$\frac{1}{160}$	$\frac{1}{160}$	3.2432e-06	1.9913	3.1504e-06	1.9911	3.0517e-06	1.9908

Table 5: Error for different h,τ and T for example 6.3

T	h	τ	$\alpha=0.8$
			$\|e^N\|$
2	$\frac{1}{100}$	$\frac{1}{100}$	6.9799e-05
4	$\frac{1}{100}$	$\frac{1}{100}$	6.0670e-04
6	$\frac{1}{150}$	$\frac{1}{150}$	9.4359e-04
8	$\frac{1}{500}$	$\frac{1}{170}$	9.1743e-04
10	$\frac{1}{1000}$	$\frac{1}{100}$	4.6852e-03

In Table (4), we report errors and order of convergence with various α. In Table (5), errors are estimated in different final time. It can be observed from table (4) and (5) that our method has higher numerical accuracy. Also Numerical and exact solutions have been demonstrated in Figure (7). In figure (9), the comparison between $u(x_j,t_k)$ and u_j^k at $t=1$ is created to show the accuracy of the presented method.

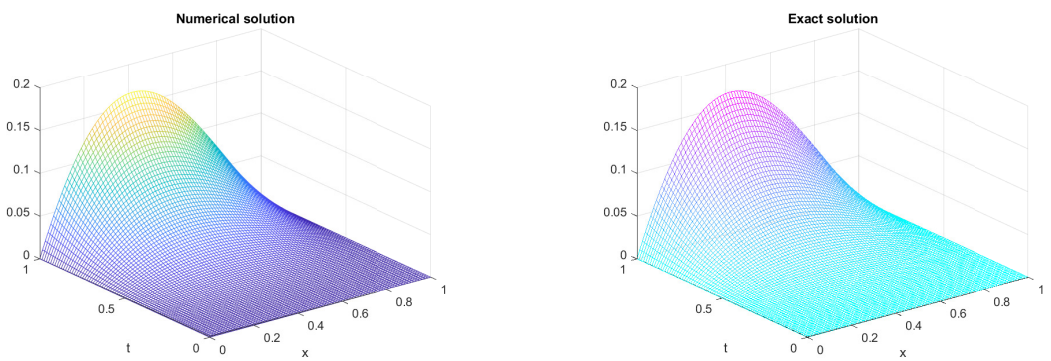

Figure 7: The plot of numerical solution (left) and exact solution (right) at $\tau=1/80$ and $h=1/80$ for example 6.3.

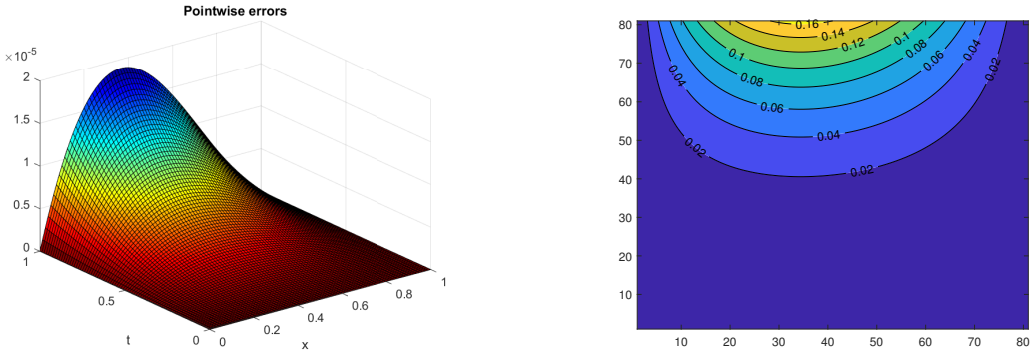

Figure 8: The plot of pointwise errors at $\tau = 1/80$ and $h = 1/80$ and contour plot of numerical solution for example 6.3.

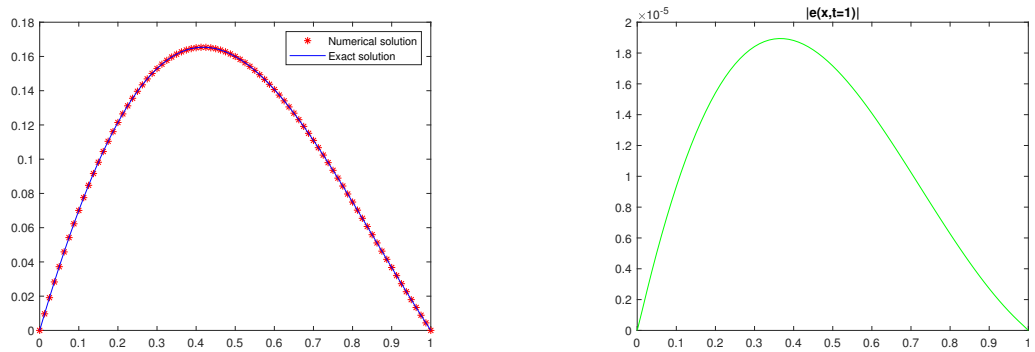

Figure 9: The comparison between numerical solution and exact solution (left) and absolute error (right) with $\tau = 1/80$ and $h = 1/80$ at $t = 1$ for example 6.3.

Example 6.4 *Consider the time fractional partial integro–differential equation* (1.1) *with initial and boundary conditions* (1.2)-(1.3) *with exact solution* $u(x,t) = t\log(x)(x-2)$, $(x,t) \in [1,2] \times [0,1]$. *The source term is taken as*

$$f(x,t) = \frac{(x-2)\log(x)t^{1-\alpha}}{\Gamma(1-\alpha)} - \frac{t(x+2)}{x^2} - \frac{4}{3}\frac{t^{\frac{3}{2}}(x+2)}{x^2}.$$

Table 6: Take $\tau = 0.01$, Error and experiment order of convergence for $\alpha = 0.2, 0.4, 0.6$ for example 6.4

h	$\alpha = 0.2$		$\alpha = 0.4$		$\alpha = 0.6$	
	$\|e^N\|$	$r_1(\tau,h)$	$\|e^N\|$	$r_1(\tau,h)$	$\|e^N\|$	$r_1(\tau,h)$
$\frac{1}{10}$	1.7336e-04		1.7351e-04		1.7440e-04	
$\frac{1}{20}$	6.0107e-05	1.5281	6.0257e-05	1.5258	6.0946e-05	1.8304
$\frac{1}{40}$	1.6378e-05	1.8758	1.6526e-05	1.8664	1.7137e-04	1.8304
$\frac{1}{80}$	4.2094e-06	1.9601	4.3569e-06	1.9234	4.9474e-06	1.7924
$\frac{1}{160}$	1.0798e-06	1.9628	1.2274e-06	1.8277	1.8148e-06	1.4469

Table 7: Error for different h, τ and T for example 6.4

T	h	τ	$\alpha = 0.6$	$\alpha = 0.8$
			$\|e^N\|$	$\|e^N\|$
2	$\frac{1}{100}$	$\frac{2}{100}$	6.3006e-06	8.0557e-06
10	$\frac{1}{100}$	$\frac{10}{100}$	2.8657e-05	2.9668e-05
20	$\frac{1}{100}$	$\frac{20}{100}$	5.6582e-05	5.7332e-05
40	$\frac{1}{100}$	$\frac{40}{100}$	1.1246e-04	1.1299e-04
80	$\frac{1}{100}$	$\frac{80}{100}$	2.2425e-04	2.2461e-04

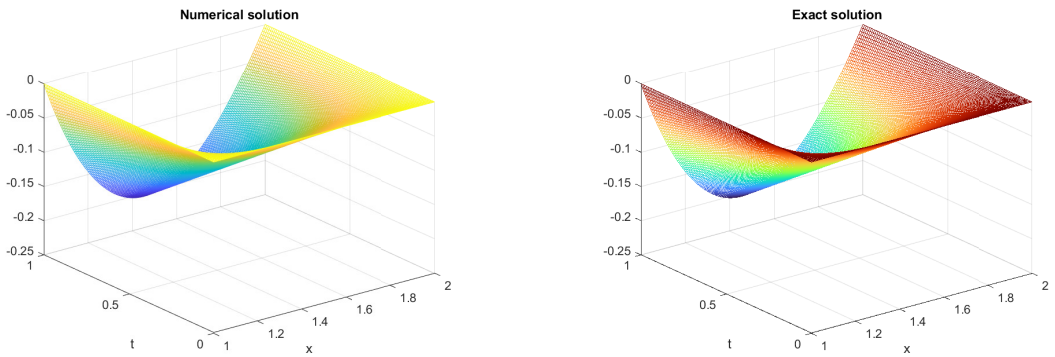

Figure 10: The plot of numerical solution (left) and exact solution (right) at $\tau = 0.01$ and $h = \frac{1}{160}$ for example 6.4.

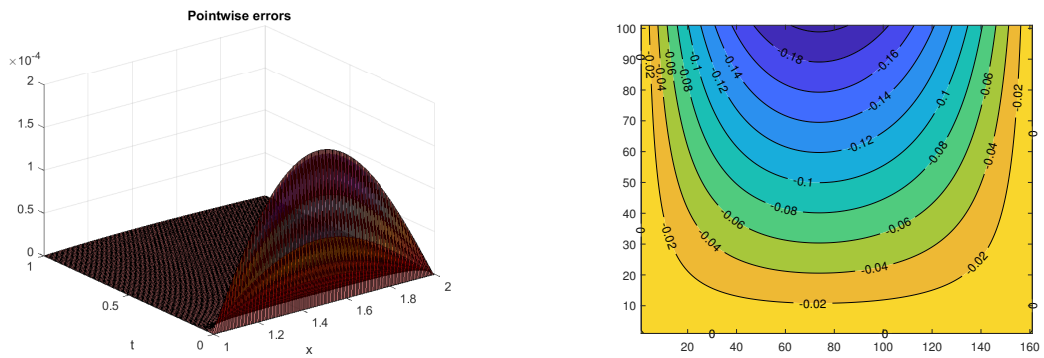

Figure 11: The plot of pointwise errors at $\tau = 0.01$ and $h = \frac{1}{160}$ and contour plot of numerical solution for example 6.4.

Tables (6),(7) *and figures* (10)-(12) *shows that the scheme works properly.*

7. Conclusions

In this article, we constructed a difference scheme using cubic B–spline Quasi–interpolation for the solution of a time fractional partial integro–differential equation with a weakly singular kernel. The time fractional derivative of the mentioned equation is approximated by a scheme of order $O(\tau^2)$ and spatial derivative replaced with a second–order approximation. We proved that the scheme is stable and convergent for $\alpha \in (0, 1)$. Several numerical examples have been carried out to show the convergence orders and efficiency of the method.

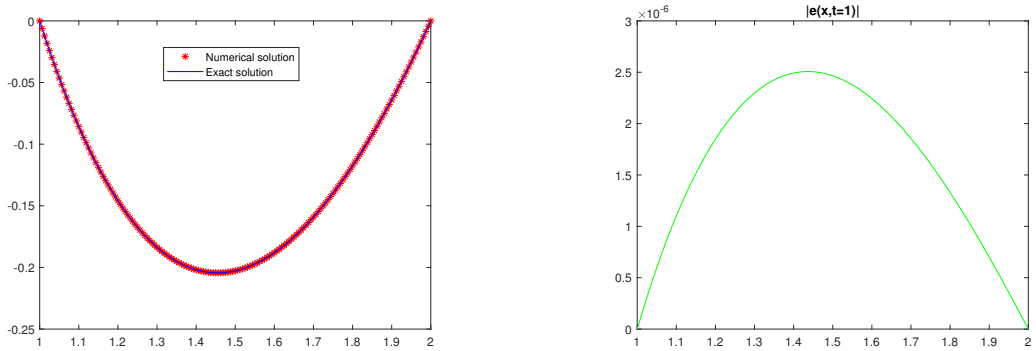

Figure 12: The comparison between numerical solution and exact solution (left) and absolute error (right) with $\tau = 0.01$ and $h = \frac{1}{160}$ at $t = 1$ for example 6.4.

References

1. Miller, K. S., Ross, B., *An introduction to the fractional calculus and fractional differential equations*, Wiley, (1993).
2. Oldham, K., Spanier, J., *The fractional calculus theory and applications of differentiation and integration to arbitrary order*, Elsevier, (1974).
3. Diethelm, K., *The Analysis of Fractional Differential Equations: An Application-Oriented Exposition Using Differential Operators of Caputo Type*, Springer, (2010).
4. Hilfer, R., *Applications of fractional calculus in physics* , World scientific, (2000).
5. Atanguna, A., *Fractional Operators with Constant and Variable Order with Application to Geo-Hydrology*, Academic Press, (2018).
6. Oliveira, E. C. D., *Solved Exercises in Fractional Calculus*, Springer International Publishing, (2019).
7. Ortigueira, M. D., *Fractional calculus for scientists and engineers*, Springer Science & Business Media, (2011).
8. Podlubny, I., *Fractional Differential Equations*, Academic Press, (1998).
9. Caponetto, R., *Fractional order systems: modeling and control applications*, World Scientific, (2010).
10. Sandev, T., Tomovski, Z., *Fractional Equations and Models: Theory and Applications*, Springer Nature, (2019).
11. Singh, H., Kumar, D., Baleanu, D., *Methods of Mathematical Modeling* , CRC Press, Taylor & Francis Group, (2020).
12. Valério, D., Costa, J. S. D., *An introduction to fractional control*, IET, (2013).
13. Damarla, S. K., Kundu, M., *Fractional Order Processes: Simulation, Identification, and Control*, CRC Press, (2018).
14. Yang, Y., Zhang, H. H., *Fractional Calculus with its Applications in Engineering and Technology*, Morgan & Claypool, (2019).
15. Tarasov, V. E., *Handbook of Fractional Calculus with Applications, Volume 4, part A*, De Gruyter, (2019).
16. Tarasov, V. E., *Handbook of Fractional Calculus with Applications, Volume 4, part B*, De Gruyter, (2019).
17. Machado, J. A. T., *Handbook of Fractional Calculus with Applications, Volume 7, part A*, De Gruyter, (2019).
18. Machado, J. A. T., *Handbook of Fractional Calculus with Applications, Volume 8, part B*, De Gruyter, (2019).
19. Băleanu, D., Lopes, A. M., *Handbook of Fractional Calculus with Applications, Volume 7, part A*, De Gruyter, (2019).
20. Tarasov, V. E., *Handbook of Fractional Calculus with Applications, Volume 7, part B*, De Gruyter, (2019).
21. Uchaikin, V. V., *Fractional derivatives for physicists and engineers*, Berlin: Springer, (2013).
22. Kumar, D., Singh, J., *Fractional Calculus in Medical and Health Science*, CRC Press, (2020).
23. Dutta, H., Akdemir, A. C., Atangana, A., *Fractional Order Analysis: Theory, Methods and Applications*, Wiley, (2020).
24. Li, C., Cai, M., *Theory and numerical approximations of fractional integrals and derivatives*, Siam, Society for Industrial and Applied Mathematics, (2019).
25. J. Zhao, J. Xiao, Y. Xu, *A finite element method for the multiterm time-space Riesz fractional advection–diffusion equations in finite domain*, Abstract and Applied Analysis, Hindawi, (2013).

26. A. Chakraborty, B.R. Kumar, *Finite element method for drifted space fractional tempered diffusion equation*, Journal of Applied Mathematics and Computing, 61, 1-19, (2019).

27. Y. Jiang, J. Ma, *High-order finite element methods for time-fractional partial differential equations*, Journal of Computational and Applied Mathematics, **235**, 3285-3290, (2011).

28. C. Li, F. Zeng, *Finite difference methods for fractional differential equations*, International Journal of Bifurcation and Chaos, **22**, 1230014-28, (2012).

29. Li, C., Zeng, F., *Numerical methods for fractional calculus*, Chapman and Hall/CRC, (2015).

30. S. Vong, P. Lyu, X, Chen, S.L, Lei, *High order finite difference method for time-space fractional differential equations with Caputo and Riemann-Liouville derivatives*, Numerical Algorithms, **72**, 195-210, (2016).

31. L. Zhao, W. Deng, J.S. Hesthaven, *Spectral methods for tempered fractional differential equations*, Journal of Computational Physics, **293**, 157–172, (2015)

32. Q. Xu, Z. Zheng, *Spectral Collocation Method for Fractiona Differential/Integral Equations with Generalized Fractional Operator*, International Journal of Differential Equations, Hindawi, (2019).

33. Owolabi, K. M., Atangana, A., *Numerical Methods for Fractional Differentiation*, Springer Singapore, (2019).

34. Daftardar-Gejji, V., *Fractional Calculus and Fractional Differential Equations*, Springer Singapore, (2019).

35. Strikwerda, J. C., *Finite difference schemes and partial differential equations*, Siam, (2004).

36. Li, Z., Qiao, Z., Tang, T., *Numerical solution of differential equations: introduction to finite difference and finite element methods*, Cambridge University Press, (2017).

37. I.J. Schoenberg, *Contributions to the problem of approximation of equidistant data by analytic functions* , Quarterly of Applied Mathematics, **4** (2), pp.112-141, (1946).

38. Schumaker, L., *Spline functions: basic theory* , Siam Society for Industrial and Applied Mathematics Philadelphia, (2015).

39. Schumaker, L., *Spline functions: basic theory* , Wiley Interscience (New York), (1981).

40. Hollig, K., Horner, J., *Approximation and modeling with B–splines* , SIAM, (2013).

41. Liouville, J. L., *Memoire sur le changement de la variable dans le calcul des differentielle a indices quelconques*, Journal de L'École Polytechnique, **15** (24), 17-54, (1835).

42. Yang, X. J., *General Fractional Derivatives: Theory, Methods and Applications*, Chapman and Hall/CRC, (2019).

43. Linz, P., *Analytical and numerical methods for Volterra equations* , Society for Industrial and Applied Mathematics, (1985).

44. Mohebbi, A, *Compact finite difference scheme for the solution of a time fractional partial integro–differential equation with a weakly singular kernel*, Mathematical Methods in the Applied Sciences, **40** 18, 7627-39, (2017).

45. Abbaszadeh, M., Dehghan, M., *A finite-difference procedure to solve weakly singular partial integro–differential equation with space-time fractional derivatives*, Engineering with Computers, 1-10, (2020).

46. Qiu, W., Xu, D., Guo, J., *Numerical solution of the fourth-order partial integro–differential equation with multi-term kernels by the Sinc-collocation method based on the double exponential transformation*, Applied Mathematics and Computation, 392, p.125693, (2020).

47. Wang, Z., Cen, D., Mo, Y., *Sharp error estimate of a compact L1-ADI scheme for the two-dimensional time-fractional integro–differential equation with singular kernels*, Applied Numerical Mathematics, 159, 190-203, (2020).

48. Qiao, L., Xu, D., Wang, Z., *An ADI difference scheme based on fractional trapezoidal rule for fractional integro–differential equation with a weakly singular kernel*, Applied Mathematics and Computation 354, 103-114, (2019).

49. Xu, D., Qiu, W., Guo, J., *A compact finite difference scheme for the fourth-order time-fractional integro–differential equation with a weakly singular kernel*, Numerical Methods for Partial Differential Equations, **36** (2), 439-458, (2020).

50. Singh, S. P., *Approximation theory, wavelets and applications*, Springer Science Business Media, (2013).

51. Tian, W., Zhou, H., Deng, W., *A class of second order difference approximations for solving space fractional diffusion equations*, Mathematics of Computation, **84** (294), 1703-1727, (2015).

52. Wang, Z., Vong, S.,*Compact difference schemes for the modified anomalous fractional sub–diffusion equation and the fractional diffusion–wave equation*, J. Comput. Phys, 277, 1-15, (2014).

53. Tang, T., *A finite difference scheme for a partial integro–differential equations with a weakly singular kernel*, Appl Numer Math, ,11:309-319, (1993).

54. Wang, J., Liu, T., Li, H., Liu, Y., He, S., *Second-order approximation scheme combined with H1- Galerkin MFE method for nonlinear time fractional convection-diffusion equation*, Computers & Mathematics with Applications, 73, 1182-1196, (2017).

Mehran Taghipour,
Department of Applied Mathematics and Computer Science, Faculty of Mathematical Sciences,
University of Guilan, P.O. Box 1914, Rasht 41938, Iran,
Rasht, Iran.
E-mail address: mtp20222@yahoo.com

and

Hossein Aminikhah (Corresponding Author),
Department of Applied Mathematics and Computer Science, Faculty of Mathematical Sciences,
Center of Excellence for Mathematical Modelling, Optimization and Combinational Computing (MMOCC),
University of Guilan, P.O. Box 1914, Rasht 41938, Iran,
Rasht, Iran.
E-mail address: aminikhah@guilan.ac.ir